멤브레인(Membrane Journal)
Vol. 17, No. 3 September, 2007, 244-253

광촉매 공정에 의한 유기물 제거가 나노여과 공정에 미치는 영향

최 인 환*,** · 김 인 철* · 민 병 렬** · 이 규 호*,†

*한국화학연구원 분리막다기능소재연구센터, **연세대학교 화학공학과
(2007년 9월 10일 접수, 2007년 9월 18일 채택)

Investigation of Photocatalytic Process on Removal of Natural Organic Matter in Nanofiltration Process

In-Hwan Choi*,, In-Chul Kim*, Byoung-Ryul Min**, and Kew-Ho Lee*,†**

*Membrane & Separation Research Center, Korea Research Institute of Chemical Technology, P.O. Box 9, Daedeog-Danji, Yusung, Taejon 305-606, Korea

**Department of Chemical Engineering, Yonsei University, 134 Shinchon-dong, Seodaemun-Gu, Seoul 120-749, Korea
(Received September 10, 2007, Accepted September 18, 2007)

요 약: 광촉매 반응이 자연유기물에 의한 나노여과막의 오염에 미치는 영향을 살펴보았다. 광촉매 분해공정은 자연유기물의 분해와 변형에 효율적이었으며 이산화티타늄과 고정화 비드를 광촉매로 사용하였다. 광촉매적 특성을 비교하기 위하여 칼슘 이온 존재 시의 휴민산의 광분해를 모델 반응으로 설정하였다. 광분해 전에는 치밀한 막오염층이 형성되어 막오염을 가속화시킨 반면, 광분해 후에는 막오염이 크게 감소하였다.

Abstract: This research investigated the effect of a photocatalytic reaction on nanofiltration (NF) membrane fouling by natural organic matter (NOM). The photocatalytic degradation was very effective for destruction and transformation of NOM and was carried out by titanium dioxide (TiO_2) and TiO_2-immobilized bead as a photocatalyst. In order to compare their phtocatalytic properties, the photocatalytic degradation of humic acid in the presence of calcium ion was used as a model reaction. After the photocatalytic degradation the membrane fouling was dramatically decreased.

Keywords: *photocatalytic reaction, nanofiltration membrane fouling, titanium dioxide, immobilized bead*

1. Introduction

The use of membrane technologies as a water treatment technology has increased in recent years, motivated in part by more stringent water regulations. Membrane technologies can be competitive in terms of efficiency and economics for water treatment applications. Nanofiltration (NF), one of several alternative membrane filtration technologies, may offer an economically competitive process to remove natural organic matter (NOM) in the natural waters [1]. However, the NOM has caused membrane fouling. Membrane fouling results in deterioration of membrane performance (i.e. permeate flux and quality) and ultimately shortens membrane life. NOM fouling is more complicated because specific interactions between chemical functional groups on the membrane surface and those of the NOM foulants may occur. Therefore, physico-chemical characteristics of NOM foulants (charge, chemical functionality and molecular conformation) play a very important role in NOM fouling. NOM fouling of polymeric membranes was also found to be affected by the ionic composition of the feed solution [2-4]. NOM is considered as a major cause of fouling in membrane

†주저자(e-mail : khlee@pado.krict.re.kr)

filtration of surface water for production of drinking water as well as process water [5].

Several previous studies have demonstrated that NOMs, and in particular humic acids (HAs), have a major influence on the flux decline. Thorsen [5] has provided an excellent overview of membrane filtration of HAs, with particular emphasis on the use of a ultrafiltration (UF) membrane for color removal. Mallevialle et al. [6] characterized the fouling layer formed during microfiltration (MF) and UF of natural water. They reported that the fouling layer was composed mostly of clay (kaolinite) and organic matter. Furthermore, the organic matter was found to be packed under the inorganic fouling layer, forming a gel-like organic matrix. Lahoussine-Turcaud et al. [7] studied the UF of several different organic and inorganic macromolecules and concluded that organic substances like humic and tannic acids had a much greater effect on the flux decline than did the inorganic colloids. Hong and Elimelech [3] reported during NF, with the rate of flux decline controlled by the magnitude of the electrostatic interactions in combination with the hydrodynamic drag due to the filtrate flow.

Photocatalytic degradation process allows in many cases a destruction of NOM in small and harmless species, without using chemicals, avoiding sludge production. The process is based on the electronic excitation of a molecule or solid caused by electrons and adsorption that dramatically alters its ability to lose or gain electrons and promote decomposition of pollutants to harmless by-products. Alternatively, direct absorption of light by the pollutant, can lead to charge injection from the excited state of the pollutant to the conduction band of the semiconductor [8,9]. In recent years, TiO_2 based photocatalytic degradation of NOM has been extensively investigated [10]. The inhibition and competition effects on the TiO_2/UV system in the presence of NOM, different TiO_2 bands, various metal ions, anions and oxy-anions have also been studied to understand the limitations of photocatalytic degradation process [10].

Table 1. Characteristics of NF 270 Membrane

Properties	Value
Membrane Type	Polyamide Thin-Film Composite
Maximum Operating Pressure	600 psig (41 bar)
Maximum Operating Temperature[a]	104°F (40°C)
Free Chlorine Tolerance	< 0.1 ppm

[a] Maximum temperature for continuous operation above pH 10 is 95°F (35°C).

In this paper, photocatalytic degradation processes by TiO_2 and TiO_2-immobilized bead have been studied. The effect of the photocatalyst on NF membrane fouling was investigated. Surface characterization techniques provided insight into the mechanistic features associated with membrane fouling by NOM.

2. Experimental

2.1. Model Solutions

The Model solution was used as humic acid (HA, sodium salt) obtained from Aldrich (Milwaukee, WI). Stock solution was prepared by dissolving HA (0.1 g/L) in deionized water and anhydrous calcium chloride (Junsei) was added in the HA solution.

2.2. NF Membrane Properties

A commercially available NF membrane was NF-270 (Dow-FilmTec Corp., Midland, MI). The properties of the NF 270 membrane are presented in Table 1. Performance experiments were carried out at 70 psi after running for 30 min using aqueous solutions containing 500 mg/L of NaCl, 500 mg/L of $CaCl_2$, and 2000 mg/L of $MgSO_4$, respectively. The salts for membrane characterization were purchased from Junsei. The flow rate and temperature of the feed solution were 3 L/min and 25°C, respectively.

A cross-flow membrane test unit consisted of a rectangular membrane cell, a pressure gauge, a thermo-controller, a flow-meter, and a high-pressure pump (Hydracell pump, Model-13, Wanner Engineering, USA) (Fig. 1). The area of the membrane cell was about

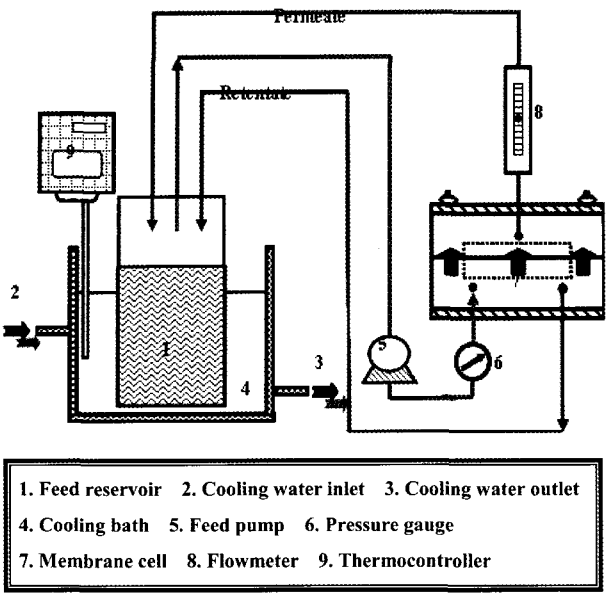

Fig. 1. Schematic description of membrane filtration unit.

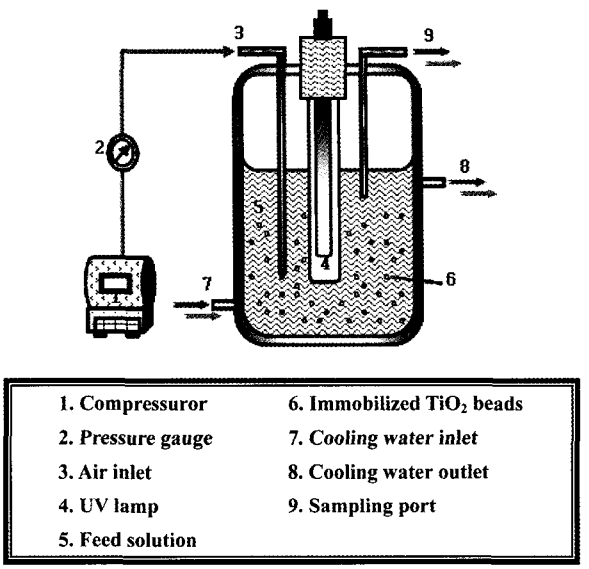

Fig. 2. Experimental setup for photocatalytic degradation process.

Table 2. Fabrication Condition of P25-immobilized Beads

Immobilized bead	1% bead	3% bead	5% bead	7% bead	9% bead	12% bead
PSf	12	12	12	12	12	12
NMP	34	34	34	34	34	34
MC	34	33	32	31	30	29
PEG600	19	18	17	16	15	13
TiO_2 content (%)	1	3	5	7	9	12
Coagulation temperature	25°C	25°C	25°C	25°C	25°C	25°C

35.36 cm^2. All membrane experiments were carried out at a feed pressure of 40~50 psi, a feed flow rate of 3 L/min and a temperature of 25°C. An initial water flux was constantly maintained at 1.0 m^3/m^2day. The flux was normalized by dividing flux with time (J) by the initial water flux (J_0).

2.3. Photocatalytic Degradation Process

TiO_2 powder (P25) was purchased from Degussa. In order to immobilize P25, the P25 particles were dispersed in the mixed solvent containing N-methyl-2-pyrrolidone (NMP, Merck), 2-methoxyethanol (MC, Sanchun), polyethylene glycol 600 (PEG 600, Junsei) by a ball-mill. A desired amount of polysulfone (PSf, BASF) was added in the slurry. The compositions of the casting solution were presented in Table 2. The polymer solution was transferred to a syringe and dropped into deionized water.

Photocatalytic degradation experiments were conducted in a 6 L hollow cylindrical glass reactor (Fig. 2). The inner hollow tube is made of quartz with 8 W, 365 nm UV-lamp (Philips) placing inside the hollow tube to provide the irradiation source. The light source used herein was a low-pressure mercury lamp. In order to improve the efficiency of the photocatalyst, hydrogen peroxide (Duksan) was used as an oxidant agent. HA concentrations were evaluated using an OPTIZEN 2120 UV/Vis spectrophotometer (MECASYS Co.) at an absorbance of UV_{254}.

2.4. Analytical Methods

The surface of the NF membrane was analyzed by

Table 3. Performance of an NF 270 Membrane

Salts	Flux (m^3/m^2day)	Rejection (%)	Concentration (mg/L)	Pressure (psi)	Temperature (°C)
NaCl	1.82	70	500	70	25
$CaCl_2$	1.86	50	500	70	25
$MgSO_4$	1.38	98.5	2,000	70	25

SEM, ATF-FT-IR, and AFM. All samples were dried overnight at room temperature. The SEM micrographs were obtained using JSM-1025A SEM (JEOL). The ATR-FT-IR technique (Perkin-Elmer 2000) was used to investigate functional groups and molecular structures on the membrane surface and deposited foulants. The AFM technique was used to image membrane surface with a nanometer scale resolution. The topographic images were obtained from an NanoScope® IV Scaning Probe (Microscope Controller Digital Instruments, Veeco Metrology Group, USA).

3. Results and Discussions

3.1. NF Membrane Properties

The membrane used in this study has features of typical NF membranes, as shown in Table 3. In other words, the NF membrane has a moderate passage for monovalent ions and a high retention for divalent ions. It has been known that one of the most important properties of the NF membranes are their ability to fractionate ionic mixtures. A low passage for multivalent ions is combined with a moderate retention for monovalent ions. These observation of the NF membranes can be explained by the Donnan equilibrium and size exclusion. The separation of ions can be determined by the interaction between the membrane surface charge and the ions. In addition, the retention difference of ions can be explained by the effective size difference between the membrane pore size and the hydrated ions [11-13].

3.2. NF Membrane Fouling

Previous studies have reported that an increase in ion strength, especially in the form of divalent cations (Ca^{2+} and Mg^{2+}) can decrease surface charge and subsequently result in a reduced rejection of inorganic ions [3,14-16].

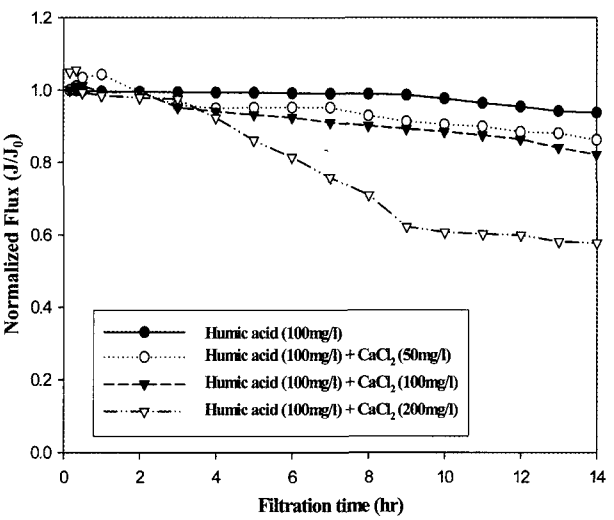

Fig. 3. Effect of calcium concentration on NOM fouling: humic acid concentration, 100 mg/L; feed pressure, 40~50 psi; feed flow rate, 3 L/min; temperature, 25°C.

Divalent cations can form metal-humic complexes due to more effectively charge screening and therefore have a greater effect on reducing the negative charge of HA. As a result of the reduced interchain electrostatic repulsion due to neutralization of negative charges of functional groups, humic acid molecules form a small, coiled conformation, and subsequently a more compact fouling layer.

Fig. 3 clearly shows the effect of NOM on membrane fouling increase as the concentration of calcium ion increases. The HA without calcium ions was observed to improve the initial flux in the pH range 6~7 and the flux decline hardly occurred. It was considered that the fouled layer might have loose structure because there does not exist calcium ion which binds different HA. Adsorbed HA onto the membrane surface resulted in an increase in hydrophilicity of the membrane surface within 1 hr, and permeate flux was

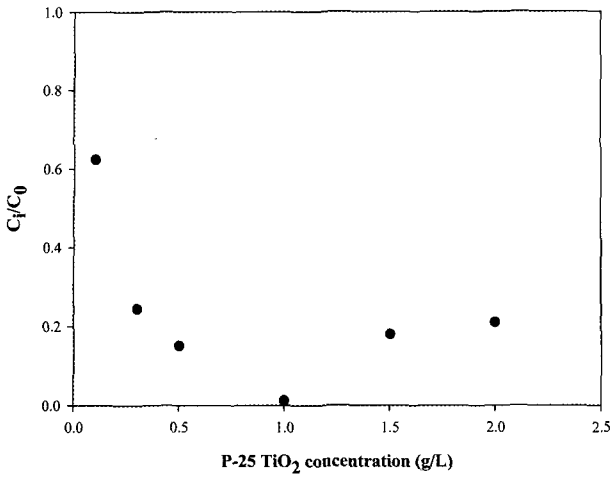

Fig. 4. Effect of the P25 TiO_2 concentration on the photocatalytic degradation of humic acid.

slightly enhanced [3]. After 3 hrs running, the decrease in permeate flux was caused by promoted concentration polarization. When 50 and 100 mg/L calcium ions were present, the flux declined by 15% and 18% for 14 hrs, respectively. In the presence of 200 mg/L calcium ions, the flux decline extremely decreased by 42%. The average rejection for UV_{254} and color were found to be 98 and 99%, respectively.

3.3. Photocatalytic Degradation Process

The influence of the photocatalyst concentration on the photocatalytic kinetics of HA solution has been investigated employing different concentrations of P25 varying from 0.1 to 2 g/L (Fig. 4). For higher concentrations of TiO_2, the removal efficiencies decreased with increasing amount of TiO_2. These results show that there is an optimum amount of TiO_2. Above this concentration level (1 g/L), the suspended TiO_2 particles block UV-light passage and reduce the formation of electron/hole pairs and active sites [10]. Most likely, the turbidity and colour of treated solution, along with the effect of TiO_2 blocking in solution, made the decomposition less effective.

To solve the problem of photocatalyst recovery, the particles were immobilized onto the polymer. A suitable diameter for bead was around 3 mm. Fig. 5 shows a SEM image of the surface of the immobilized

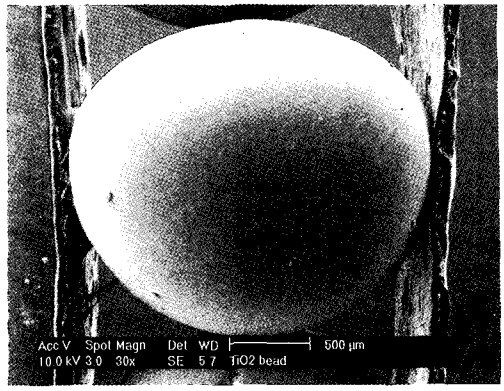

(a)

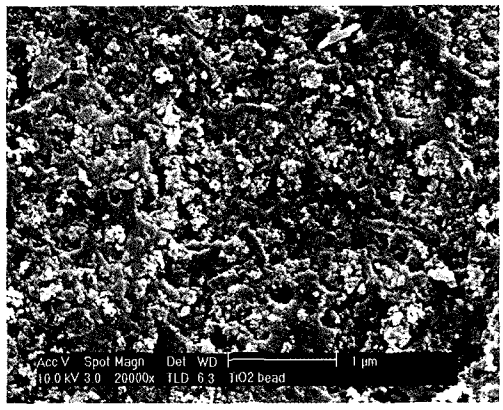

(b)

Fig. 5. SEM images of P25-immobilized beads: (a) a bead: (b) magnification of a bead.

bead. The image of Fig. 5(a) illustrates that immobilized bead shows a spherical shape and a diameter of immobilized TiO_2 bead is approximately 2.5~3 mm. The image of Fig. 5(b) shows that the particles with the size of 30~40 nm are present on the polymer.

Fig. 6 shows that the photocatalytic degradation in suspended system are more efficient than immobilized system. In the case of suspended system, the surface of the photocatalyst is only active if the photocatalyst is illuminated. It is difficult to illuminate all the photocatalysts in the suspended system, because the photocatalyst further away from the light source are shielded from the radiation of the photocatalyst near the light source. Hence, the penetration depth of light into suspension is limited. In the immobilized system, it is possible to obtain a configuration in which all the cata-

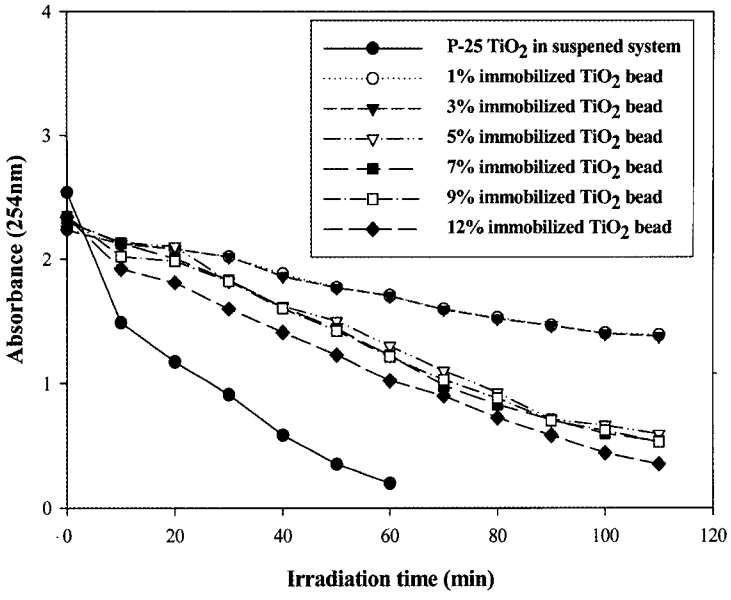

Fig. 6. Photocatalytic degradation of humic aicd by the P25-immobilized beads.

lysts are illuminated. But, a disadvantage of this system is that mass transfer limitation can easily occur [17,18].

To investigate the effect of TiO_2 concentration on the immobilized beads, TiO_2 content was varied from 1 to 12%. As TiO_2 content increased, the photocatalytic degradation efficiency is increased. The photocatalytic degradation efficiency of unimmobilized particles after 60 min was much higher than that of immobilized beads because of the buried particles in the polymer for immobilized beads.

3.4. Effect of Photocatalytic Degradation on NF Membrane Fouling

The photocatalytic degradation prior to the use of NF membrane process was performed to mitigate membrane fouling for a total period of 60 min. The photocatalyst degraded about 90% of the initial HA. The photocatalytic degradation of HA resulted in considerable fouling mitigation. During the photocatalytic degradation, the reactive functional groups associated with humic substances were replaced by new functional groups with lower sorption affinities for the membrane surface. Additionally, major breakdown of NOM macromolecules caused a substantial decrease in hydrophobic interactions with membrane surface, resulting in lower adsorptive organic fouling. An important consideration in adsorptive membrane fouling could be the charge density of NOM. An increase in organic acid constituents of NOM after the photocatalytic degradation provides more ligands or sites for calcium complexation, and consequently the negative charge of NOM decreases [19]. Such a decrease in NOM charge may promote adsorptive organic fouling for the negatively charged membranes. Nonetheless, the lower fouling tendency of the photocatalytic degraded water, based on the permeate fluxes shown in Fig. 7, suggested that decreased hydrophobic interaction due to lower adsorption affinity was more influential than a reduction in charge repulsions between the NOM molecules and membrane surface. It must be noted that the hydrogen bonding energies associated with adsorption of hydrophobic NOM on membrane surfaces are generally much larger than the electrostatic potential energies associated with charge interactions. The photocatalytic degradation of HA by the immobilized TiO_2 beads leads to prevent calcium ion from reacting with the carboxylic acid of humic acid and the membrane.

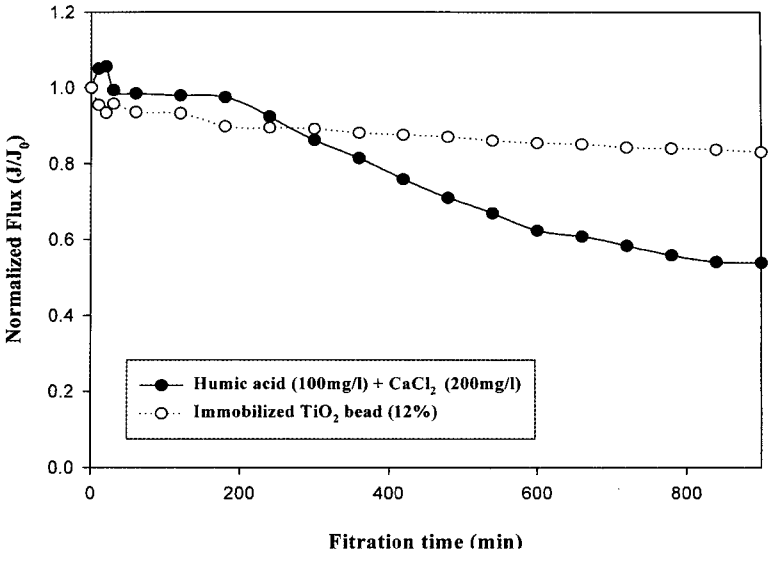

Fig. 7. Effect of photocatalysis by the P25-immobilized beads on nanofiltration membrane fouling.

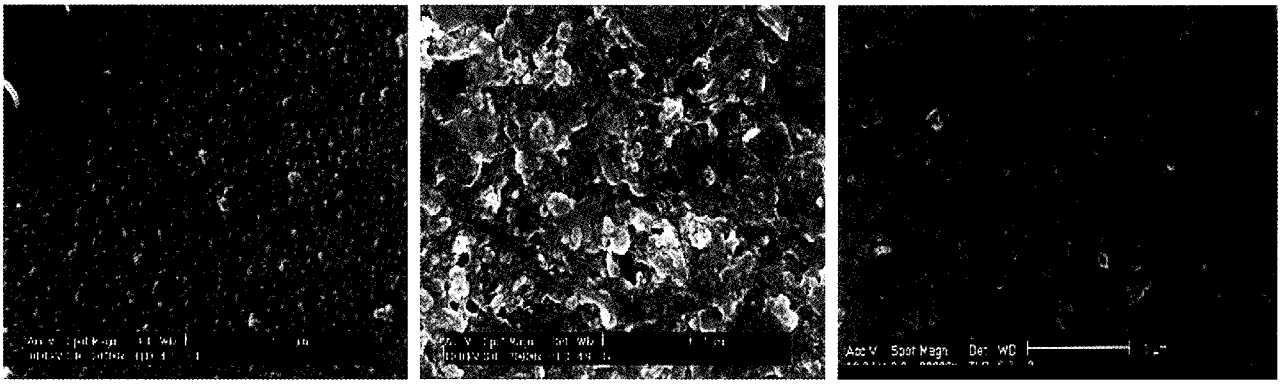

(a) (b) (c)

Fig. 8. SEM images for (a) virgin membrane (b) fouled membrane (humic acid (100 mg/L) and $CaCl_2$ (50 mg/L)) (c) membrane after photocatalysis.

3.5. Analysis of Membrane Surface

In order to further identify the nature of the NOM fouling, the SEM images of NF membrane surface after 18 hrs filtration were obtained. From Fig. 8, the SEM image of the virgin membrane (Fig. 8(a)) exhibited a typical polyamide layer, while the images of fouled membranes showed the deposition of the foulants on the membrane surface (Fig. 8(b)). When the HA was degraded by the photocatalyst, the membrane was found to be much less fouled (Fig. 8(c)).

The FT-IR spectra of a virgin membrane and fouled membranes were shown in Fig. 9. The virgin membrane reflects the typical pattern of polyamide or polysulfone membranes [20,21]. The FT-IR spectra for the fouled membranes indicate that the absorption peaks in the virgin membrane spectra were apparently disappeared due to fouled materials. The band between wave numbers of 950 and 1,200 cm^{-1} were significantly shown for the fouled membrane. The peak apparently originated from the polysaccharides in NOM can be the C-O-C vibrations of polysaccharides at frequencies of 1,050 and 1,080 cm^{-1} [20]. The FT-IR spectra for membrane after photocatalysis were slightly decreased in intensity, as compared to those for the virgin membrane. These observations supported that NOM foulants were predominantly smaller organic acids removable

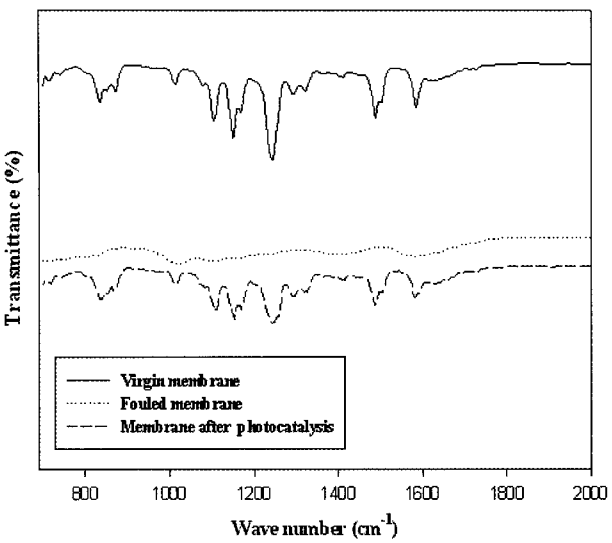

Fig. 9. FT-IR spectra of nanofiltration membranes; (a) virgin membrane; (b) fouled membrane (humic acid (100 mg/L) and $CaCl_2$ (50 mg/L)); (c) membrane after photocatalysis.

by photocatalytic degradation.

The AFM images are presented in Fig. 10. Significant differences are observed between the surface morphologies of the virgin and fouled membrane in terms of their root mean square (rms) surface roughness values. The virgin membrane exhibits surface roughness of 30 nm (Fig. 10(a)), which is significantly lower than the values (129 nm) for fouled membranes (Fig. 10(b)). During the initial stages of filtration, macromolecules such as humic or hydrophobic NOM fraction as well as less negatively charged NOM constituents (such as calcium-bound NOM) preferentially deposit onto the negatively charged membrane surface. The surface roughness (Fig. 10(c)) after photocatalysis is slightly higher (60 nm) than that of virgin membrane. It seems that photocatalysis of the HAs results in decreased possibility of ionic bridge between the NF membrane and HA.

4. Conclusions

The fouling layer formed in the presence of Ca^{2+} is very compact and highly resistant to hydrodynamic forces. The photocatalytic degradation of humic acid

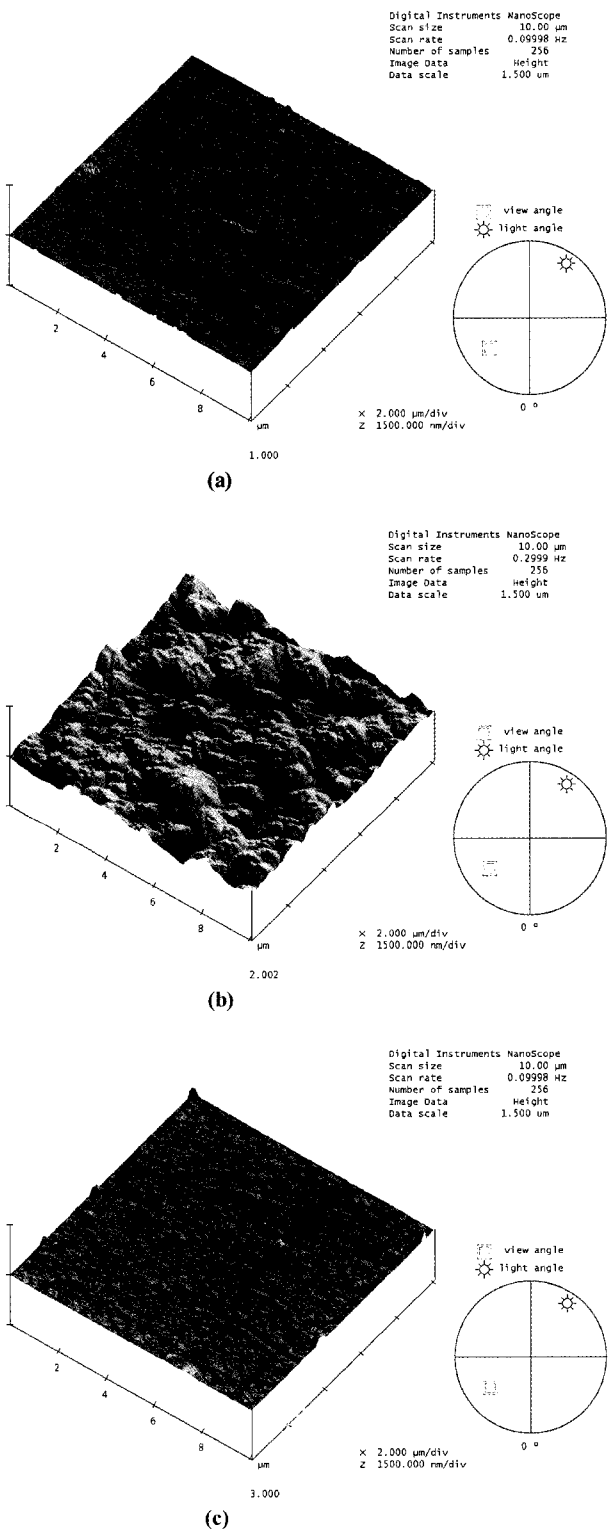

Fig. 10. AFM images of nanofiltration membranes; (a) virgin membrane; (b) fouled membrane (humic acid (100 mg/L) and $CaCl_2$ (50 mg/L)); (c) membrane after photocatalysis.

significantly mitigated nanofiltration membrane fouling. These results could be confirmed by ATR-FTIR, AFM, and SEM. The P25 particles were successfully immobilized onto polymer. The photocatalytic activity increased as the concentration of TiO_2 in immobilized beads increases. The phtocatalytic process using immobilized beads was useful for a pretreatment of nanofiltration.

References

1. A. I. Schafer, A. G. Fane, and T. D. Waite, "Nanofiltration of natural organic matter: removal, fouling and the influence of multivalent ions", *Desalination*, **118**, 109 (1998).
2. A. Braghetta, F. A. DiGiano, and W. P. Ball, "NOM accumulation at NF membrane surface: impact of chemistry and shear", *J. Environ. Eng. Div. ASCE*, **124**, 1087 (1998).
3. S. Hong and M. Elimelech, "Chemical and physical aspects of natural organic matter (NOM) fouling of nanofiltration membranes", *J. Membr. Sci.*, **132**, 159 (1997).
4. M. M. Clark and P. Lucas, "Diffusion and partitioning of humic acid in a porous ultrafiltration membrane", *J. Membr. Sci.*, **143**, 13 (1998).
5. T. Thorsen, "Removal of humic substances with membranes system, use and experiences", *Proceedings of membrane technology conference on American Water Works Association*, 131, (1993).
6. J. Mallevialle, C. Anselme, and O. Marsigny, "Effects of humic substances on membrane processes, in: I. H. Suffet and P. MacCarthy (Ed.), Aquatic Humic Substances: Influence onFate and Treatment of Pollutants", ACS, Washington DC, pp. 749-767 (1989).
7. V. Lahoussine-Turcaud, M. R. Wiesner, and J. Y. Bottero, "Fouling in tangential-flow ultrafiltration: effect of colloid size and coagulation pretreatment", *J. Membr. Sci.*, **52**, 173 (1990).
8. L. Sanchez, J. Peral, and X. Domenech, "Photocatalyzed destruction of aniline in UV-illuminated aqueous TiO_2 suspensions", *Electrochimica. Acta*, **42(12)**, 1877 (1997).
9. D. Chen and A. K. Ray, "Photodegradation kinetics of 4-nitrophenol in TiO_2 suspension", *Water Res.*, **32(11)**, 3223 (1998).
10. M. Bekbolet, A. S. Suphandag, and C. S. Uyguner, "An investigation of the photocatalytic efficiencies of TiO_2 powders on the decolourisation of humic acids", *J. Photochem. Photobiol. A: Chem.*, **148**, 121 (2002).
11. A. Yaroshchuk and E. Staude, "Charged membranes for low pressure reverse osmosis properties and applications", *Desalination*, **86(2)**, 115 (1992).
12. R. J. Petersen, "Composite reverse osmosis and nanofiltration membranes: Review", *J. Memb. Sci.*, **83**, 81 (1993).
13. A. Braghetta, "The influence of solution chemistry operating conditions on nanofiltration of charged and uncharged organic macromolecules", Ph.D. Dissertation, Univ. of North Carolina, Chapel Hill (1995).
14. M. Nyström, L. Kaipia, and S. Luque, "Fouling and retention of nanofiltration membranes", *J. Membr. Sci.*, **98**, 249 (1995).
15. W. Wei and A. L. Zydney, "Humic acid fouling during ultra-filtration", *Environ. Sci. Technol.*, **34**, 5043 (2000).
16. J. W. Cho, G. Amy, and J. Pellegrino, "Membrane filtration of natural organic matter: comparison of flux decline, NOM rejection, and foulants during filtration with three UF membranes", *Desalination*, **127**, 283 (2000).
17. D. F. Ollis, E. Pelizzetti and N. Serpone, "Photocatalyzed destruction of water contaminants", *Environ. Sci. Technol.*, **25(9)**, 1522 (1991).
18. A. K. Ray and A. A. C. M. Beenackers, "Novel swirl-flow reactor for kinetic studies of semiconductor photocatalysis", *AIChE J.*, **43(10)**, 2571 (1997).
19. M. S. Chandrakanth and G. L. Amy, "Effects of NOM source variations and calcium complexation

capacity on ozone-induced particle destabilization", *Water Res.*, **32(1)**, 115 (1998).

20. A. Pihlajamäki, P. Väisänen, and M. Nyström, "Characterization of clean and fouled polymeric ultrafiltration membranes by Fourier transform IR spectroscopy-attenuated total reflection", *Colloids Surf. A Physicochem. Eng. Aspects*, **138(2-3)**, 323 (1998).
21. H. Zhu and M. Nyström, "Cleaning results characterized by flux, streaming potential and FTIR measurements", *Colloids Surf. A Physicochem. Eng. Aspects*, **138(2-3)**, 309 (1998).